Green Chemical Technology

SCIEPublish

Article

Feasibility of Combining Novel LacN with Traditional Enzyme Immobilization Techniques: Further Enhancement of Enzyme Activity and Stability

Zhaobo Wang [1,*], Dajun Ren [2] and Ruan Chi [1,3]

[1] Phosphogypsum Utilization R&D Center, Hubei Three Gorges Laboratory, Yichang 443007, China; rac@wit.edu.cn (R.C.)

[2] College of Resource and Environmental Engineering, Wuhan University of Science and Technology, Wuhan 430081, China; dj_ren@163.com (D.R.)

[3] School of Resources and Safety Engineering, Wuhan Insititute of Technology, Wuhan 430073, China

* Corresponding author. E-mail: wangzhaobo@hbsxsys.com (Z.W.)

Received: 23 June 2026; Revised: 24 July 2026; Accepted: 28 August 2026; Available online: 11 September 2026

ABSTRACT: Laccase-inorganic hybrid nanoflowers (LacN) represent a novel enzyme immobilization strategy. The integration of this approach with traditional adsorption-based immobilization offers a novel and efficient pathway for laccase immobilization. In this study, LacN was immobilized onto two types of Cu/HAP-BC (natural mineral-derived Cu/nHAP-BC and porcine bone-derived Cu/pHAP-BC) to synthesize LacN@Cu/HAP-BC. Single-factor experiments, combined with Box-Behnken response surface methodology, were used to optimize the immobilization parameters. The optimal preparation conditions were determined as 60% LacN suspension, pH 6.0, reaction time of 2 h for LacN@Cu/nHAP-BC; and 80% LacN suspension, pH 6.0, reaction time of 2 h for LacN@Cu/pHAP-BC. Multiple characterizations confirmed uniform anchoring of flower-like LacN on porous Cu/HAP-BC. Compared with free laccase, LacN@Cu/HAP-BC showed significantly improved stability: after 30 d of storage, LacN@Cu/nHAP-BC and LacN@Cu/pHAP-BC retained 81.35% and 76.70% of their initial activities, respectively (*vs.* 42.98% for free laccase); the thermal half-lives ($t_{1/2}$) at 65 °C were 502 min and 433 min, respectively, approximately 3.0–3.5 times that of free laccase (142 min). Additionally, the two composites retained 71.98% and 80.15% of their initial activity after 10 consecutive catalytic cycles, showing satisfactory reusability. These results verify that the composites deliver favorable storage, thermal, and cyclic stability, acting as a feasible biocatalyst candidate for lab-level water treatment and biomass conversion. Further tests on continuous reactors and real wastewater pollutants are needed to confirm its industrial applicability.

Keywords: Laccase nanoflowers; Copper based carrier; Enzyme immobilization; Enzyme activity; Stability

1. Introduction

Laccase (Lac) is a polyphenol oxidase (ρ-diphenol oxidase, EC 1.10.3.2) containing four copper ions. Since water is the sole byproduct of its catalytic reaction, Lac is regarded as an eco-friendly enzyme with extensive applications in bioresource processing and environmental remediation. In particular, Lac plays a key role in the pretreatment of lignocellulosic biomass and the degradation of recalcitrant pollutants (e.g., chlorophenols, azo dyes) in industrial wastewater [1,2]. However, the practical application of Lac is hindered by poor stability, susceptibility to environmental factors, and the inability to be recycled. Therefore, there is an urgent need to improve its stability and reusability for industrial applications. Laccase nanoflower (LacN) technology is a novel immobilization strategy. LacN forms a rose-like morphology through coordination of laccase with copper ions and phosphate, thereby enhancing enzyme tolerance and catalytic activity due to its nanoscale architecture and copper-mediated electron transfer [3]. Since its inception, the enzyme-inorganic hybrid nanoflower preparation strategy has garnered significant attention across diverse fields, including biotechnology, biomedical materials, chemical engineering, and dye decolorization [4]. However, the practical application of LacN is limited by its nanoscale dimensions, which make recovery and reuse difficult in large-scale systems.

Enzyme immobilization on insoluble supports (e.g., by adsorption, cross-linking, or covalent binding) can preserve catalytic activity, enhance stability, and confer reusability. A recent comprehensive review systematically categorized mainstream laccase immobilization matrices into organic polymers, single inorganic minerals, and organic–inorganic hybrid composites, and summarized their respective strengths and limitations in stabilizing laccase and degrading emerging refractory contaminants [5]. Among various hybrid carrier systems, biochar-hydroxyapatite composites exhibit distinctive merits, including hierarchical porous structure, tunable metal active sites, and low-cost waste feedstock. Metal organic Frameworks (MOFs) have also been proven to construct favorable catalytic microenvironments via strong coordination with enzymes, effectively locking protein structures and extending catalytic service life in complex reaction systems [6]. In our previous studies, laccase was successfully immobilized on biochar and hydroxyapatite-based composites with improved stability [7–12]. Importantly, Jiang et al. showed that copper-based supports can enhance laccase activity by 1.7-fold. Given the recovery bottleneck for LacN and the advantages of immobilization, integrating LacN with a suitable support is a promising strategy [13].

Hydroxyapatite (HAP) is an excellent host material for enzyme immobilization. It can be derived from natural minerals, biological sources (e.g., animal bones), or chemical synthesis [14]. HAP has a well-ordered hexagonal structure that allows substitution of Ca^{2+} by Cu^{2+} to form Cu/HAP [15,16]. However, Cu/HAP suffers from poor stability under acidic conditions. To address this, our previous studies [17–19] synthesized a Cu/HAP-biochar composite (Cu/HAP-BC) with enhanced specific surface area and stability. This composite exhibits an enhanced specific surface area, improved physicochemical properties, and a copper-ion mediated activation mechanism, which collectively contribute to the potential retention of higher enzymatic activity and stability.

Therefore, in this study, we immobilized LacN onto Cu/HAP-BC supports to synthesize LacN@Cu/HAP-BC via a physicochemical-biological synergistic strategy. The main objectives were to optimize the synthesis conditions and to evaluate the enhanced enzymatic activity and stability of the composite. This work aims to provide a practical immobilized laccase platform for bioresource and environmental applications, particularly in wastewater treatment and biomass valorization.

2. Materials and Methods

2.1. Materials and Reagents

Hydrochloric acid, sodium hydroxide, copper sulfate pentahydrate, acetic acid, sodium acetate, sodium chloride, potassium chloride, sodium dihydrogen phosphate, potassium dihydrogen phosphate, Coomassie Brilliant Blue G-250, and bovine serum albumin (BSA) were purchased from Sinopharm Chemical Reagent Co., Ltd. (Shanghai, China). Hydroxyapatite (HAP) was derived from two sources: a synthetic source (purchased as nHAP) and a biological source (extracted from porcine bone, denoted as pHAP). Laccase was purchased from Sigma-Aldrich (St. Louis, MO, USA).

2.2. Optimization of the Synthesis of LacN@Cu/HAP-BC

2.2.1. Synthesis of Laccase-Inorganic Hybrid Nanoflowers (LacN)

LacN was synthesized according to a previously reported method with slight modifications, adopting a 100-fold scaled-up reaction system that retains the original volume ratio of laccase buffer and $CuSO_4$ solution [3]. Briefly, 300 mL of laccase-phosphate buffer solution (1 mg/mL, pH 7.4) was added to 2 mL of $CuSO_4$ solution (120 mM) to obtain the LacN suspension under optimal conditions. The mixture was then incubated in a constant temperature shaker at 25 °C for three d and stored for subsequent use.

2.2.2. Preparation of Cu/HAP-BC Supports

Cu/HAP-BC supports (Cu/nHAP-BC and Cu/pHAP-BC) were prepared according to our previous protocol with modifications [17–19]. nHAP (4.5 μm, 99%) was purchased, while pHAP was extracted from porcine bone by alkali/acid treatment and calcination at 600 °C (Ca/P = 1.67). For copper loading, 1.0 g of HAP was mixed with Cu^{2+} (250 mg/g HAP, pH 7.0) and stirred at 45 °C for 6 h. The obtained Cu/HAP was then mixed with rape straw (Cu:HAP:straw = 1:4:15) and pyrolyzed under N_2 at 800 °C for 1.5 h to yield Cu/HAP-BC.

2.2.3. Immobilization of LacN onto Cu/HAP-BC

A single-factor experiment was conducted to optimize the immobilization conditions, investigating three key variables: LacN suspension volume fraction (20–100%), pH (4.0–8.0), and reaction time (2–10 h). For each test, 50 mL of LacN suspension was added to Cu/HAP-BC support (either Cu/nHAP-BC or Cu/pHAP-BC) in a 250 mL flask, and the mixture was incubated at 25 °C with shaking at 200 rpm. After incubation, the catalysts (denoted as LacN@Cu/nHAP-BC and LacN@Cu/pHAP-BC) were recovered by centrifugation, washed, and air-dried. The residual enzyme activity under each condition was measured to determine the optimal range for each variable.

Based on the optimal ranges identified from the single-factor experiments, a multi-factor optimization was performed using Box-Behnken response surface methodology (RSM) [20]. The three independent variables—LacN suspension volume fraction (A), pH (B), and reaction time (C)—were coded at three levels (−1, 0, +1), with catalytic activity (U) as the response value (Y). The experimental design and the coded variable levels are provided in Tables S1 and S2 (electronic supplementary material). Response surface plots were generated to analyze the interaction effects among the variables and to identify the optimal preparation conditions.

2.3. Characterization

The surface morphologies of the samples were examined using a scanning electron microscope (MIRA LMS, TESCAN a.s., Brno, Czech Republic) at an accelerating voltage of 10 kV. Transmission

electron microscope (Tecnai F20, FEI Company, Hillsboro, OR, USA) characterization was performed at 200 kV to observe the internal structure of LacN. The specific surface area and pore size distribution were measured via N_2 adsorption-desorption at 77 K using an ASAP 2460 instrument (Micromeritics Instrument Corp., Norcross, GA, USA). X-ray diffraction (XRD) patterns were recorded on a D8 Advance diffractometer (Bruker AXS GmbH, Karlsruhe, Germany) with Cu Kα radiation at 40 kV and 40 mA, with a scanning range of 2θ = 10°–80°, and a scanning rate of 5°/min. Fourier Transform Infrared (FTIR) spectra were obtained on a Nicolet iS20 spectrometer (Thermo Fisher Scientific Inc., Waltham, MA, USA) in the range of 4000–400 cm^{-1} using the KBr pellet method.

2.4. Determination of Catalytic Activity

The catalytic activity of free and immobilized laccase was assayed using 2,2′-azino-bis(3-ethylbenzothiazoline-6-sulfonic acid) (ABTS) as the substrate. Protein concentration in the supernatant was determined using the Bradford assay with bovine serum albumin (BSA) as the standard. For free laccase, 0.1 mL of enzyme solution was mixed with 2.9 mL of ABTS solution. For immobilized laccase, LacN@Cu/HAP-BC was added to 3 mL of the same ABTS solution. The reaction was carried out at 25 °C for 3 min, and the increase in absorbance at 420 nm was recorded using a UV-visible spectrophotometer. One unit (A, U) of laccase activity was defined as the amount of enzyme required to oxidize 1 μmol of ABTS per minute. The specific activity (SA, U/g) was calculated as activity per gram of catalyst. Relative activity (RA, %) was defined as the ratio of the measured activity to the maximum activity within the experimental group. All measurements were performed in triplicate. The specific calculation formulas are presented below:

$$A = \frac{10^6 \times \Delta A \times V \times f}{\varepsilon \times t} \quad (1)$$

$$SA = \frac{A}{M} \quad (2)$$

$$RA = \frac{A_i}{A_{max}} \times 100\% \quad (3)$$

The specific calculation formulas are presented below, where ΔA is the change in absorbance at 420 nm, V is the volume of the reaction system (L), f is the dilution factor, ε is the molar extinction coefficient of ABTS (36,000 $M^{-1} \cdot cm^{-1}$), t is the reaction time (min), M is the catalyst mass (mg), A_i is the measured catalytic activity (U), and A_{max} is the maximum catalytic activity within the group (U).

2.5. Determination of Enzyme Kinetic Parameters

The Michaelis-Menten kinetic parameters (K_m and v_{max}) were determined by monitoring the enzymatic reaction with ABTS as the substrate [21]. The Michaelis constant (K_m) represents the substrate concentration at which the reaction rate is half of the maximum velocity, while v_{max} is defined as the maximum reaction rate achieved under specific enzyme concentrations and reaction conditions. The enzymatic kinetics of equivalent amounts of LacN@Cu/nHAP-BC, LacN@Cu/pHAP-BC, and free laccase were investigated by measuring the catalytic rates at various ABTS concentrations over a fixed period. For comparative studies, the amounts of free laccase and immobilized laccase were adjusted to provide equivalent initial enzymatic activity units (U) in the reaction mixture, ensuring a fair comparison of their kinetic and stability properties. The kinetic parameters were estimated based on the Michaelis-Menten model, and the calculation formula is expressed as follows:

$$v = \frac{v_{max} \times [S]}{K_m + [S]} \quad (4)$$

The K_m and v_{max} values were calculated by transforming the data into a Lineweaver-Burk double reciprocal plot. The formula for the Lineweaver-Burk model is expressed as follows:

$$\frac{1}{v} = \frac{K_m}{v_{max}} \times \frac{1}{[S]} + \frac{1}{v_{max}} \quad (5)$$

The K_m and v_{max} values were calculated by transforming the data into a Lineweaver-Burk double reciprocal plot, where v represents the reaction rate (U), S is the substrate concentration (μmol/L), v_{max} is the maximum reaction rate (U), and K_m is the Michaelis-Menten constant (mM).

2.6. Determination of Enzyme Stability

Enzymatic reactions typically require mild conditions and are highly susceptible to factors such as temperature, pH, and storage conditions; thus, enzyme stability—encompassing storage stability, pH stability, thermal stability, and reusability—is a critical parameter reflecting tolerance to extreme external environments. Storage stability was evaluated by storing LacN@Cu/HAP-BC and equivalent free laccase at 4 °C for 30 d, measuring activity every three d (in triplicate), and calculating relative activity with the maximum value defined as 100%. pH stability was determined by incubating samples in buffers of varying pH (3.0–9.0) for 2 h, while thermal stability and thermal inactivation kinetics were investigated by incubating samples at temperatures ranging from 25 to 75 °C for 2 h; for both stability tests, residual activity was measured in triplicate, and relative activity was calculated with the maximum activity within each group set as 100%. Reusability was assessed over 10 consecutive cycles: after each reaction, the mixture was centrifuged for 10 min, the catalyst was washed three times, and the recovered sample was reused under identical conditions, with the relative activity calculated using the activity of the first cycle as the 100% reference. The thermal inactivation of laccase is generally described as a "one-step, two-state" process, where the active form converts to an inactive form via a first-order monomolecular irreversible reaction [22]. This process is typically modeled using first-order kinetics. Specifically, the thermal tolerance test was conducted by incubating LacN@Cu/HAP-BC and an equivalent amount of free laccase in a water bath at 65 °C for 0–2 h, with samples withdrawn every 20 min. The relative activity was calculated with the maximum catalytic activity within each group defined as 100%. The first-order thermal inactivation kinetic equation and the half-life formula are expressed as follows:

$$\ln\frac{A_t}{A_0} = \ln A = -kt \quad (6)$$

$$t_{1/2} = \frac{\ln 2}{k} \quad (7)$$

where A_t is the catalytic activity measured at time t (U), A_0 is the initial catalytic activity within the experimental group (U), t is the reaction time (min), and k is the deactivation rate constant (min^{-1}).

3. Results and Discussion

3.1. The Influence of Different Factors on Laccase Activity

The experimental results presented in Figure 1a,b demonstrate that the catalytic activity of both LacN@Cu/nHAP-BC and LacN@Cu/pHAP-BC initially increased with the volume fraction of the LacN suspension, reaching a peak before slightly declining. This trend can be attributed to the limited number of available adsorption sites on the Cu/HAP-BC support. In the initial stage, increasing the LacN volume fraction enhances the binding efficiency with these sites, thereby boosting catalytic activity. However, once the adsorption sites are saturated, excess LacN tends to aggregate on the surface, potentially masking active sites and hindering contact between the enzyme and substrate, as well as electron transfer, thereby leading to a slight reduction in activity. The relative activity of LacN@Cu/nHAP-BC remained

at 100.00% within a volume fraction range of 60–80%, indicating this as the optimal interval. Under single-factor conditions, a volume fraction of 60% was selected as it achieved maximum activity while minimizing LacN dosage. For LacN@Cu/pHAP-BC, the relative activity increased from 94.90% to 100.00% between 60% and 80%, but then decreased significantly to 79.34% at 100% due to aggregation effects. Thus, 60–80% was determined as the optimal range for LacN@Cu/pHAP-BC, with the highest activity observed at 80%. To ensure a single variable in subsequent experiments, the LacN suspension volume fractions were fixed at 60% for LacN@Cu/nHAP-BC and 80% for LacN@Cu/pHAP-BC.

Subsequently, the effect of pH (ranging from 4.0 to 8.0) was investigated. Free laccase typically exhibits optimal activity within a specific acidic pH range, and deviations can cause denaturation or irreversible inactivation, limiting its industrial application. However, as shown in Figure 1c,d, both LacN@Cu/nHAP-BC and LacN@Cu/pHAP-BC maintained high catalytic activity across the pH range of 4.0–8.0, with a maximum activity loss of only 25.83%. This broadened pH tolerance is attributed to the dual protection provided by the LacN nanoflower structure and the biochar support, which shields the enzyme's active center. Notably, the composites exhibited maximum activity under near-neutral conditions, making them more suitable for industrial use. Further analysis identified pH 5.0–7.0 as the optimal range, where the relative activities were 80.86–100.00% for LacN@Cu/nHAP-BC and 86.98–100.00% for LacN@Cu/pHAP-BC. Since both composites achieved their maximum activity at pH 6.0 under single-factor conditions, this value was selected for subsequent experiments.

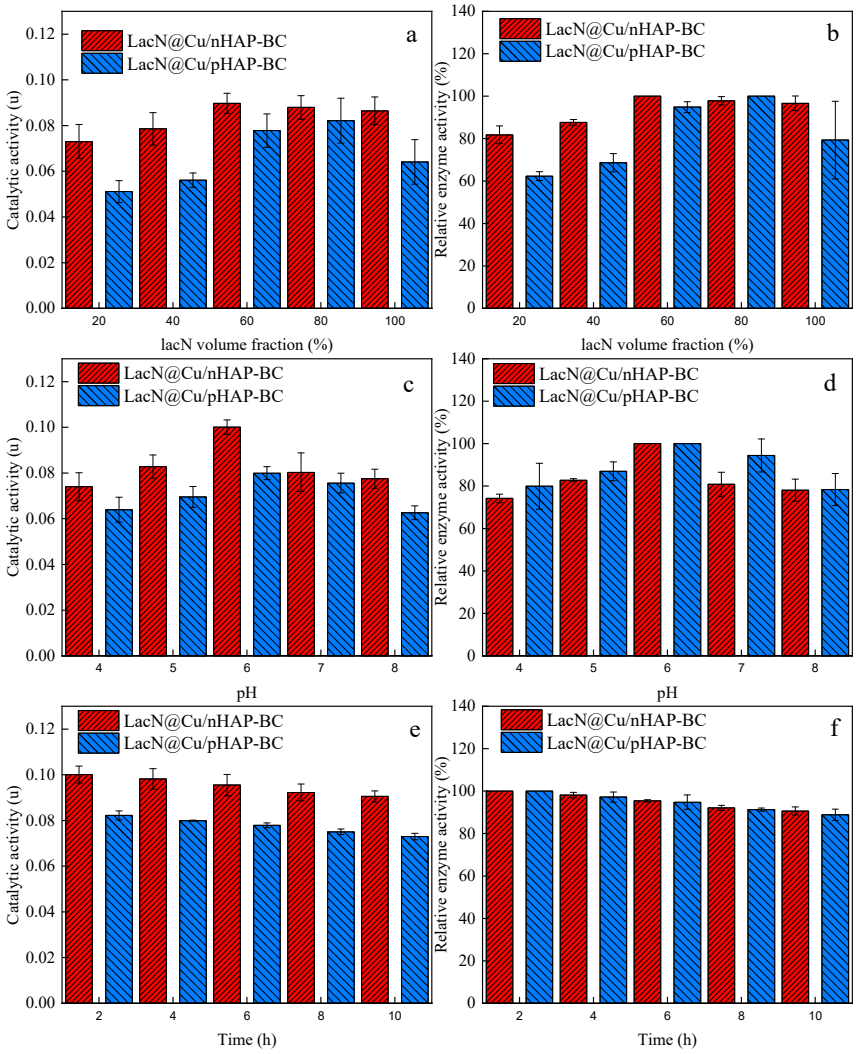

Figure 1. Effect of different factors on the catalytic activity of immobilized LacN: (**a**,**b**) LacN volume fraction, (**c**,**d**) pH, and (**e**,**f**) reaction time.

Finally, the effect of reaction time (2–10 h) on immobilization efficiency was evaluated (Figure 1e,f). The results indicate that the catalytic activity of LacN@Cu/nHAP-BC was slightly higher than that of LacN@Cu/pHAP-BC, and both followed a similar trend: activity decreased gradually with prolonged reaction time. This phenomenon is presumably due to the desorption of partially bound LacN from the adsorption sites on Cu/HAP-BC over extended periods. Collectively, the optimal reaction time range for both LacN@Cu/nHAP-BC and LacN@Cu/pHAP-BC was determined to be 2–4 h.

3.2. Optimization of the Synthesis of LacN@Cu/HAP-BC

3.2.1. Model Fitting and Matching

Upon inputting the experimental data, a comprehensive statistical analysis was performed to evaluate various models, including linear, two-factor interaction (2FI), quadratic, and cubic models. In statistical theory, a p-value less than 0.0500 indicates model significance, with lower values denoting higher significance (derived from the F-value). Additionally, an R^2 value closer to 1 signifies a better fit between the predicted and actual values. As shown in Table S3 in the electronic supplementary material, the linear and 2FI models were deemed insignificant for LacN@Cu/nHAP-BC. Although the linear and 2FI models for LacN@Cu/pHAP-BC yielded p-values < 0.0500, they were rejected due to their low R^2 values, which deviated significantly from 1. Conversely, both the quadratic and cubic models for both composites exhibited extremely low p-values (<0.0001) and R^2 values close to 1. However, the cubic model was discarded as the coefficients of the high-order terms were too small to be expressed as a practical equation. Consequently, the quadratic model was selected as the most suitable fit, as it accurately reflects the relationship between catalytic activity and the independent variables.

Table S4 in the electronic supplementary material presents the parameter estimates and confidence analysis derived from the quadratic model under coded conditions, where A, B, and C represent LacN suspension volume fraction, pH, and reaction time, respectively. The coefficient estimates indicate the expected change in response per unit change in a factor, assuming all other factors remain constant. The intercept in the orthogonal design represents the overall mean response of all experiments, while the coefficients represent adjustments around this mean based on factor settings. A Variance Inflation Factor (VIF) of 1 indicates orthogonality between factors; a VIF > 1 suggests multicollinearity, though values < 10 are generally acceptable. As observed in Table S4, the VIF values for all factors were approximately 1, confirming the orthogonality of the experimental design. Analysis of the coefficient magnitudes revealed that for LacN@Cu/nHAP-BC, both the LacN suspension volume fraction (A) and pH (B) exerted a negative effect on catalytic activity, with pH having a more pronounced impact. Reaction time (C) demonstrated a negligible effect. These findings are consistent with the results obtained from the single-factor experiments.

For LacN@Cu/nHAP-BC, the interaction effects of the factors on catalytic activity were ranked as follows: $B^2 > BC > AC > AB > A^2 > C^2$. Among these, the interaction terms AB, AC, and BC exhibited positive effects, while the quadratic terms A^2, B^2, and C^2 showed negative effects. Conversely, the results for LacN@Cu/pHAP-BC differed: both LacN suspension volume fraction (A) and pH (B) exerted positive effects on catalytic activity, with volume fraction having a more pronounced impact, whereas reaction time (C) showed a negative but negligible effect. These observations are consistent with the single-factor experimental results. The interaction effects for LacN@Cu/pHAP-BC were ranked as: $B^2 > C^2 > A^2 > AB > AC > BC$. Specifically, A^2, C^2, and AC were positive effects, while AB, B^2, and BC were negative effects. Based on the selected quadratic model, Figure 2 presents the correlation between the actual and predicted catalytic activities for both composites. The 17 sets of experimental data points align closely along a straight line, indicating a satisfactory model fit and high reliability of the predicted values.

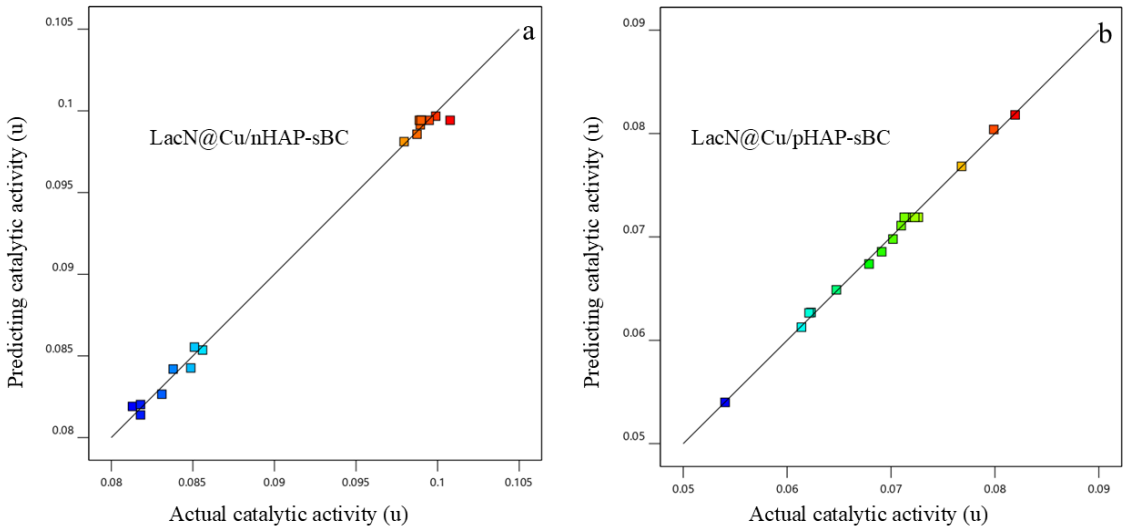

Figure 2. Relationship diagram between actual catalytic activity and predicted catalytic activity: (**a**) LacN@Cu/nHAP-BC; (**b**) LacN@Cu/pHAP-BC.

3.2.2. Response Surface Analysis

The reaction time was fixed at the midpoint (3 h) to analyze the interaction effect between LacN suspension volume fraction and pH on the immobilized enzyme activity, as illustrated in Figure 3a,b. It can be observed that pH exerted a significant influence on both LacN@Cu/nHAP-BC and LacN@Cu/pHAP-BC. The catalytic activity increased initially and then decreased, indicating that maintaining an intermediate pH level yields higher activity. Regarding the LacN suspension volume fraction, its effect on LacN@Cu/nHAP-BC was relatively minor (Figure 3a). Within the range of 60–80%, the catalytic activity of LacN@Cu/nHAP-BC remained stable; however, considering cost-effectiveness, a lower volume fraction is preferred for the preparation process. Conversely, as depicted in Figure 3b, the volume fraction had a more pronounced impact on LacN@Cu/pHAP-BC, with higher dosage corresponding to higher catalytic activity.

With the pH fixed at the midpoint (pH 6.0), Figure 3c,d illustrates the interaction effects between LacN suspension volume fraction and reaction time on catalytic activity. While the volume fraction exerted similar influences on both composites, distinct behaviors were observed: LacN@Cu/nHAP-BC maintained stable activity within the 60–80% range, whereas the activity of LacN@Cu/pHAP-BC increased with higher dosages, consistent with the single-factor results. Furthermore, reaction time had a negligible impact on both catalysts; activity remained stable before slightly declining with prolonged incubation. This phenomenon is attributed to the desorption of partially bound LacN from the adsorption sites on Cu/HAP-BC over extended periods. Finally, with the LacN suspension volume fraction fixed at the midpoint (70%), Figure 3e,f presents the interaction effects between pH and reaction time. The response surface plots indicate that activity initially increased and then decreased with pH, while reaction time showed a slight downward trend, consistent with the single-factor experiments. To precisely determine the optimal conditions for LacN immobilization onto Cu/HAP-BC, the model equations were further derived using the Box-Behnken response surface methodology.

Experimental design and optimization were performed using the Box-Behnken response surface methodology (RSM). The resulting quadratic model equations for LacN@Cu/nHAP-BC and LacN@Cu/pHAP-BC are expressed as follows:

For LacN@Cu/nHAP-BC:

$$Y = -0.44 + 0.000056A + 0.18B - 0.0062C + 0.00003AB + 0.000053AC + 0.00065BC - 0.0000030A^2 - 0.016B^2 - 0.0002C^2$$

For LacN@Cu/pHAP-BC:

$$Y = -0.22 - 0.00024A + 0.090B - 0.0065C - 0.000042AB + 0.000027AC - 0.00029BC + 0.0000083A^2 - 0.0069B^2 + 0.00089C^2$$

In summary, the optimal preparation conditions determined for LacN@Cu/nHAP-BC were: LacN suspension volume fraction of 60%, system pH of 6.0, and reaction time of 2 h. For LacN@Cu/pHAP-BC, the optimal conditions were: LacN suspension volume fraction of 80%, system pH of 6.0, and reaction time of 2 h.

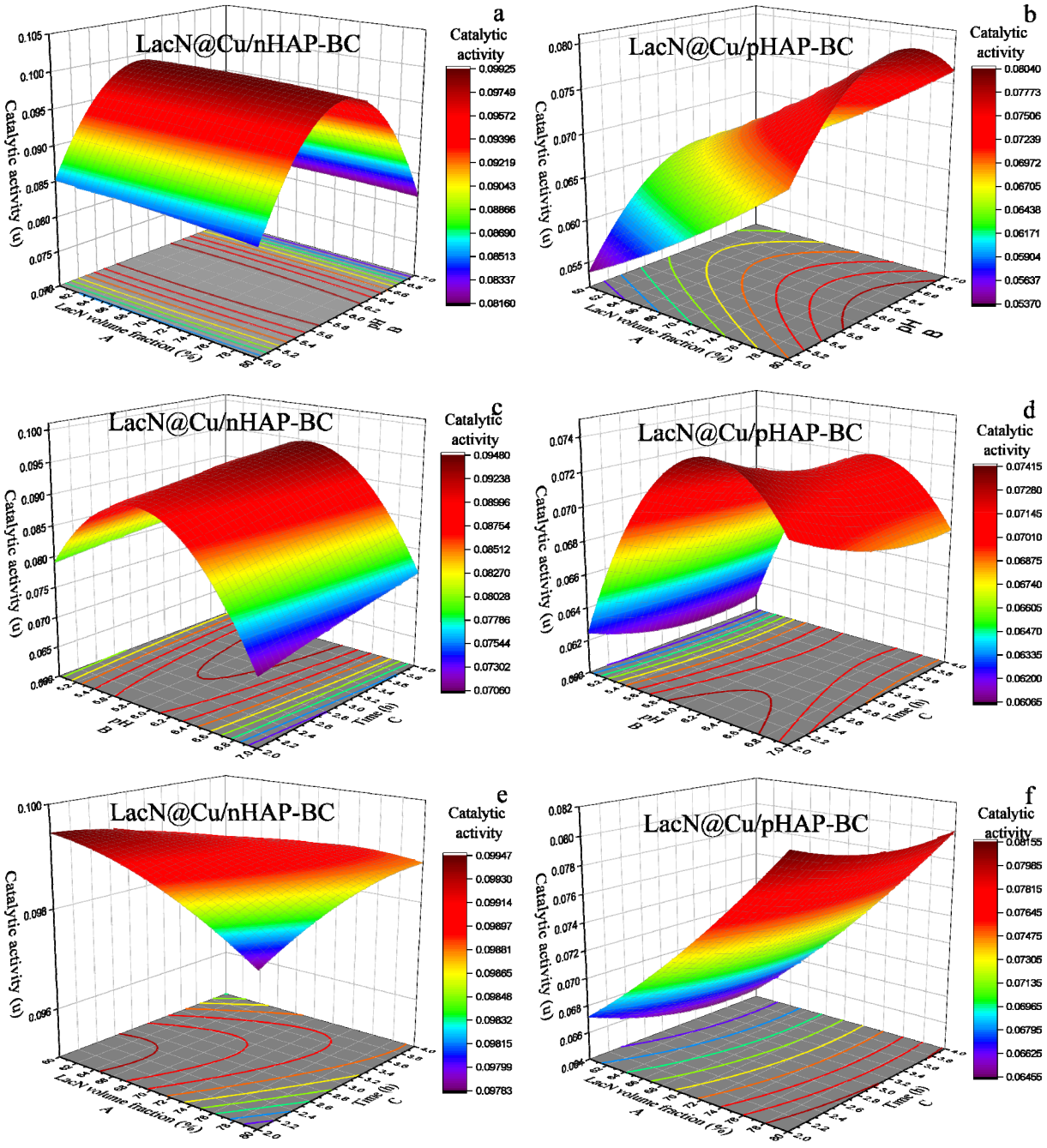

Figure 3. Box-Behnken response surface plots illustrating the effects of (**a**,**b**) LacN suspension volume fraction and pH, (**c**,**d**) LacN suspension volume fraction and reaction time, and (**e**,**f**) pH and reaction time on enzyme activity.

3.3. Characterization

3.3.1. SEM Analysis

The SEM images of the laccase-inorganic hybrid nanoflowers (LacN) are presented in Figure 4a. It can be observed that the aggregation and anisotropic growth of laccase molecules and primary copper phosphate crystals led to the formation of a branched flower-like structure. A high concentration of laccase molecules increases the number of nucleation sites, allowing the crystals to grow to larger dimensions [3]. Figure 4b displays the TEM image of LacN. The striking similarity in their nested structures confirms that this layered nanoflower architecture is achieved through strong coordination and electrostatic interactions between Cu^{2+} and laccase molecules [23], thereby effectively immobilizing the laccase molecules within the copper phosphate crystal core. Consequently, LacN can expose the laccase active centers, enhance the affinity between the enzyme and the substrate, and provide a larger contact area, thereby facilitating improved catalytic activity. The SEM images clearly reveal a honeycomb-like structure resembling rose petals. The formation mechanism involves two main steps: (1) Interactions occur between amino acids in the laccase molecules and Cu^{2+}, which combine with the primary crystals formed by Cu^{2+}-PBS to create "petals", effectively loading the laccase within these structures; (2) During the incubation process, the crystals continuously grow, aggregate, and assemble, ultimately forming the rose-like laccase-inorganic hybrid nanoflowers (LacN).

The morphologies of the bare supports (Cu/nHAP-BC and Cu/pHAP-BC) are shown in Figure 4c,d, respectively. Both supports exhibit rough, porous surfaces with abundant pores of irregular sizes, which provide anchoring sites for subsequent LacN immobilization. The surface shows sintering and melting phenomena typical of high-temperature pyrolysis, and the bamboo-like pore structure is characteristic of biochar derived from straw biomass [24]. After LacN immobilization, the flower-like structures of LacN can be clearly observed "blooming" on the Cu/HAP-BC surface (Figure 4e for LacN@Cu/nHAP-BC and Figure 4f for LacN@Cu/pHAP-BC), confirming the successful loading of LacN onto the support.

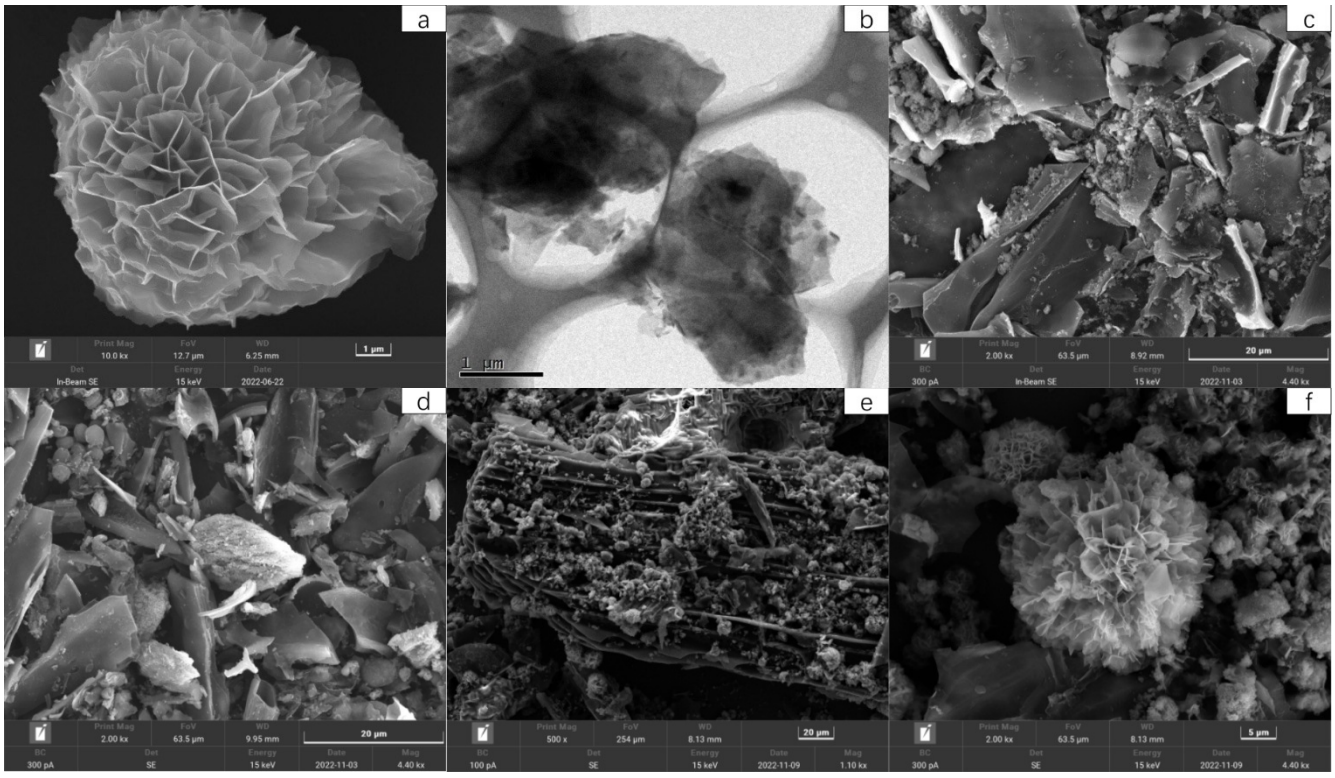

Figure 4. (**a**) SEM image (20.0 k×) and (**b**) TEM image of LacN; SEM images of (**c**) Cu/nHAP-BC and (**d**) Cu/pHAP-BC; SEM images of (**e**) LacN@Cu/nHAP-BC and (**f**) LacN@Cu/pHAP-BC.

3.3.2. BET, XRD, FTIR Analysis

The BET characterization of LacN@Cu/HAP-BC is presented in Figure 5a,b, with specific surface area and pore structure parameters listed in Table S5 of the Electronic Supplementary Material. The N_2 adsorption-desorption isotherms (Figure 5a) reveal similar trends for both LacN@Cu/nHAP-BC and LacN@Cu/pHAP-BC, characteristic of type IV isotherms indicative of mesoporous structures. The pore size distribution curves (Figure 5b) demonstrate that LacN@Cu/HAP-BC maintains a similar distribution profile to the pristine Cu/HAP-BC support. According to the data in Table S5, the specific surface areas of LacN@Cu/nHAP-BC and LacN@Cu/pHAP-BC are 168.9 m^2/g and 179.1 m^2/g, respectively, representing reductions of 102.6 m^2/g and 66.9 m^2/g compared to their respective supports. This decrease is attributed to the adsorption of LacN onto the surface and within the internal pores of Cu/HAP-BC, thereby occupying active sites and blocking the pore channels. Consequently, the total pore volumes also decreased from 0.1714 cm^3/g and 0.1727 cm^3/g (for Cu/nHAP-BC and Cu/pHAP-BC) to 0.0902 cm^3/g and 0.0963 cm^3/g, respectively. However, the average pore diameter exhibited only a slight reduction after LacN immobilization.

To investigate the immobilization of LacN, the FT-IR spectra of Cu/HAP-BC, LacN@Cu/HAP-BC, and free laccase in the range of 4000–400 cm^{-1} are displayed in Figure 5c,d. The near-identical characteristic peaks observed in Figure 5c and 5d confirm the structural consistency between nHAP and pHAP. The characteristic peaks of free laccase appear at 3426 cm^{-1}, 1645 cm^{-1}, 1360–1480 cm^{-1}, and 1025 cm^{-1}, corresponding to O–H stretching, –NH vibration, and amide I and II bands (involving C=O stretching, N–H bending, C–N stretching, and C–O–C bonds), respectively. While most peaks of Cu/HAP-BC and LacN@Cu/HAP-BC overlap, the appearance of a distinct peak at 2925 cm^{-1} in the composite, which is absent in the pure support, confirms the successful loading of laccase. This finding is consistent with similar observations reported by Lungelo Dlamini et al., who used zeolitic imidazolate frameworks as laccase carriers [25].

Figure 5e shows the XRD patterns of Cu/HAP-BC and LacN@Cu/HAP-BC, with Figure 5f displaying the standard HAP reference card. The retention of characteristic peaks matching the standard HAP pattern indicates that the integrity of the HAP crystal structure was preserved after the synthesis of LacN@Cu/HAP-BC. However, new characteristic peaks (at 45.44°) emerged in the XRD patterns of LacN@Cu/nHAP-BC and LacN@Cu/pHAP-BC after LacN loading. This phenomenon is presumably caused by the incorporation of the LacN structure, a conclusion that aligns with similar findings reported by the research group of Zhang et al. [26].

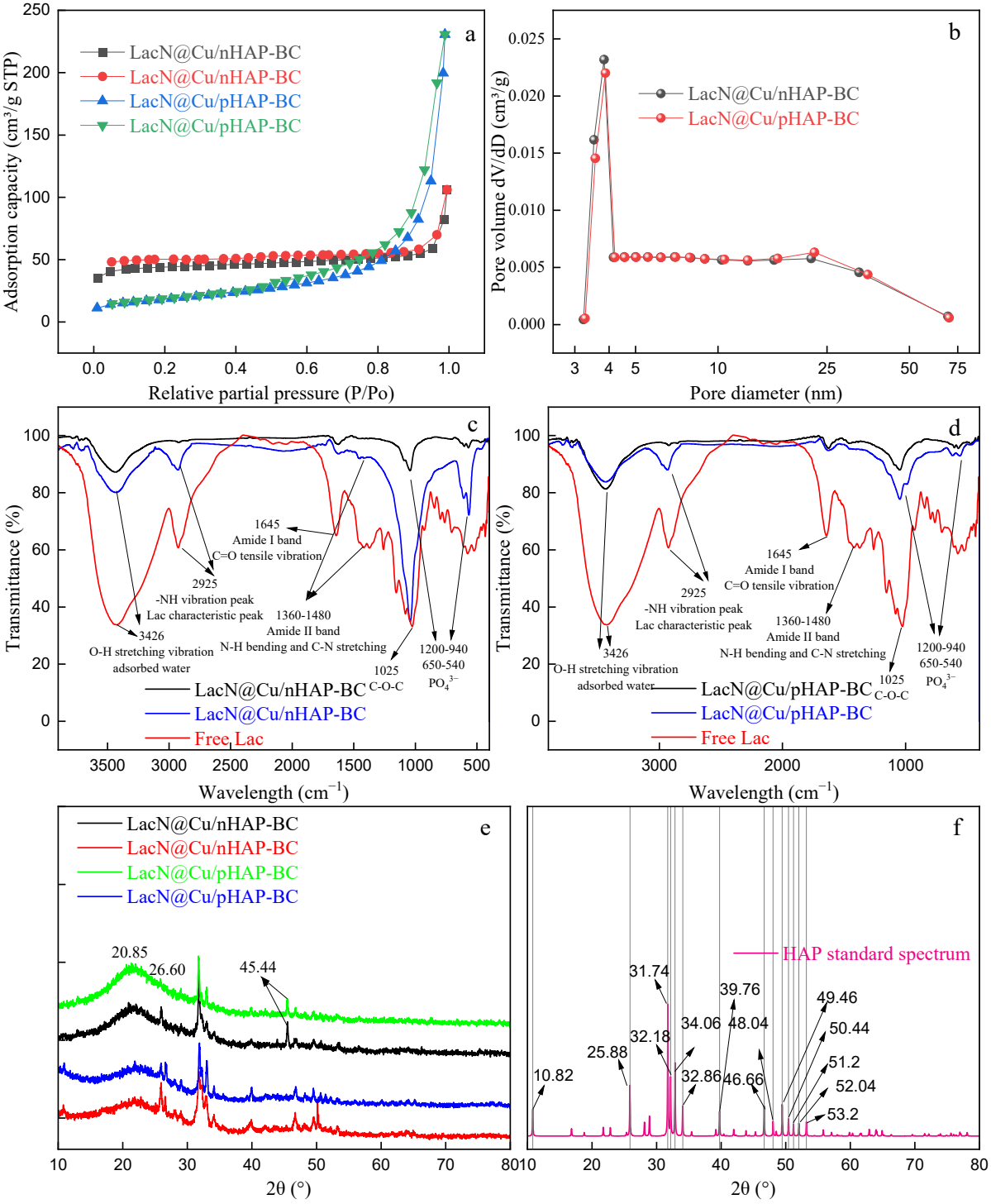

Figure 5. The BET of LacN@Cu/HAP-BC: (**a**) N_2 adsorption-desorption diagram of LacN@Cu/HAP-BC; (**b**) Pore size distribution of LacN@Cu/HAP-BC; FTIR characterization of materials before and after synthesis: (**c**) LacN@Cu/nHAP-BC; (**d**) LacN@Cu/pHAP-BC; XRD characterization of materials before and after synthesis: (**e**) XRD spectra of LacN@Cu/HAP-BC before and after synthesis; (**f**) Standard XRD spectra of hydroxyapatite.

3.4. Comparative Study on Enzyme Kinetics

The optimal preparation conditions were determined via optimization experiments. The enzymatic kinetic parameters of LacN@Cu/nHAP-BC and LacN@Cu/pHAP-BC were obtained through kinetic analysis and compared with those of free laccase to investigate the enzyme-substrate affinity and catalytic reaction rate. The kinetic parameters (K_m and v_{max}) were calculated from the slopes and

intercepts of the Lineweaver-Burk plots, respectively. The fitted Lineweaver-Burk equation parameters and kinetic data for LacN@Cu/nHAP-BC, LacN@Cu/pHAP-BC, and free laccase are summarized in Table 1. The R^2 values for all fits are greater than 0.999, indicating an excellent goodness of fit.

Table 1. Kinetic parameters of LacN@Cu/HAP-BC and free laccase (U is defined as the amount of enzyme oxidizing 1 μmol ABTS per minute).

Parameter	LacN@Cu/nHAP-BC	LacN@Cu/pHAP-BC	Free Laccase
Intercept	0.477	1.023	0.379
Slope	474.0	559.5	28.5
R^2	0.9996	0.9999	0.9986
K_m (mM)	0.99	0.55	0.075
v_{max} (U)	2.10	0.98	2.64

The Lineweaver-Burk double reciprocal plots are presented in Figure 6 in the electronic supplementary material, where the intercept represents $1/v_{max}$ and the slope represents K_m/v_{max}. The obtained data indicate that the immobilization process altered the kinetic parameters of laccase. Specifically, the v_{max} values of both LacN@Cu/HAP-BC composites were lower than that of free laccase. Among the composites, LacN@Cu/nHAP-BC exhibited a higher v_{max} (2.10 U) compared to LacN@Cu/pHAP-BC (0.98 U). Furthermore, the K_m values of LacN@Cu/HAP-BC were higher than those of free laccase, suggesting a reduced affinity for ABTS following immobilization. This phenomenon can be attributed to the adsorption of LacN onto the surfaces and within the pores of Cu/HAP-BC, which introduces mass transfer resistance and creates steric hindrance for substrate access. Similar observations have been reported in previous laccase immobilization studies, in which an increase in K_m and a decrease in activity are commonly observed after immobilization [27,28]. The reduced affinity is primarily ascribed to steric hindrance at the enzyme-substrate interface. Additionally, it may result from conformational changes in the protein structure during the immobilization process, which limit the accessibility of the active sites, thereby decreasing enzymatic activity. Although the composite catalysts sacrificed partial substrate affinity, the Cu/HAP-BC support provides abundant copper active sites and rigid spatial confinement for LacN nanoflowers. This synergistic protective effect compensates for the kinetic disadvantage, delivering far superior operational stability and recoverability compared to bare LacN nanoflowers [29]. Future parallel tests using unsupported pure LacN will further quantitatively separate the respective mass transfer contributions from nanoflower self-assembly and secondary carrier immobilization. As observed from the elevated K_m values of LacN@Cu/HAP-BC in Table 1, extra diffusion resistance mainly originates from the carrier pore channels rather than the nanoflower petals themselves, which can be further confirmed by subsequent independent LacN kinetic experiments [30].

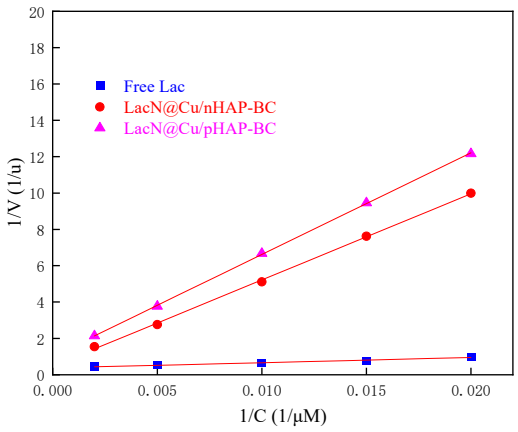

Figure 6. The Lineweaver-Burk curve.

3.5. Research on Enzyme Stability

3.5.1. Storage, Acid-Base, Reuse, Thermal Stability

pH significantly influences enzyme activity and structure by determining the ionization state of amino acids, which in turn affects the enzyme's 3D conformation and can lead to inactivation. Multi-point attachment of laccase to the support enhances its rigidity, thereby protecting it from denaturation [31]. Figure 7a evaluates the effect of pH on the enzymatic activity of LacN@Cu/HAP-BC. Compared to free laccase, the immobilized laccase exhibited higher relative activity across the pH range of 3.0–10.0. Under acidic conditions (pH 3.0), free laccase retained 50.10% of its relative activity, whereas LacN@Cu/nHAP-BC and LacN@Cu/pHAP-BC retained 60.77% and 55.20%, respectively, indicating superior acid tolerance. Both free laccase and LacN@Cu/HAP-BC achieved maximum activity at pH 5.0, consistent with the optimal working pH of laccase. Under alkaline conditions (pH 7.0–10.0), LacN@Cu/HAP-BC demonstrated significantly improved alkali tolerance compared to free laccase. While free laccase was almost completely inactivated at pH 10.0, LacN@Cu/nHAP-BC and LacN@Cu/pHAP-BC still retained 19.54% and 15.57% of their relative activities, respectively. This enhanced stability is attributed to the adsorption of laccase not only on the surface but also within the internal pores of the support. In extreme pH environments, surface-adsorbed laccase is prone to inactivation, whereas the enzyme entrapped within the internal pores is shielded and retains partial activity [8]. These results confirm that LacN@Cu/HAP-BC enhances the acid-base stability of laccase and broadens its effective working pH range. Compared with the magnetic manganese-laccase inorganic-protein hybrid system reported previously, the copper phosphate-based LacN synthesized in this work also relies on metal coordination interactions between metal ions and amino acid residues of laccase to shield the active site from structural deformation under harsh reaction environments. Different metal species bring distinct coordination strengths and catalytic synergistic effects, providing a feasible strategy to tune the environmental tolerance of immobilized laccase [32].

Free laccase is unstable and prone to deactivation during storage, which significantly limits its practical application. Enzyme immobilization is an effective strategy to improve storage stability; heterogeneous immobilized enzymes offer distinct advantages over homogeneous free enzymes, and storage stability is a critical criterion for evaluating enzyme performance [33]. To investigate the storage stability of the immobilized laccase, the enzymatic activity changes of LacN@Cu/HAP-BC and free laccase were monitored over 30 d. As shown in Figure 7b, the immobilized laccase exhibited substantially improved storage stability compared to the free form. After 15 d of storage, free laccase retained 74.72% of its activity, while LacN@Cu/nHAP-BC and LacN@Cu/pHAP-BC retained 89.43% and 84.87%, respectively. After 30 d, the relative activity of free laccase dropped to only 42.98%, whereas LacN@Cu/nHAP-BC and LacN@Cu/pHAP-BC still maintained 81.35% and 76.70% of their initial activities. These results demonstrate that LacN@Cu/HAP-BC possesses excellent storage stability. The structural stability and rigidity provided by the LacN structure and the Cu/HAP-BC support effectively protect the enzyme from unfolding and denaturation. A previous investigation of *Rhus vernicifera* laccase immobilized on magnetic nanoparticles also confirmed that inorganic solid supports can effectively prolong the enzyme's half-life and maintain residual activity during long-term storage [34].

Although free laccase exhibits strong catalytic activity towards polyphenolic substrates, its non-recyclability hinders industrial applications. Enzyme immobilization resolves this issue, with reusability being a critical performance metric [35]. The reusability of LacN@Cu/HAP-BC was evaluated over 10 reaction cycles using ABTS as the substrate (Figure 7c). Both composites demonstrated excellent operational stability, confirming that immobilization effectively endows laccase with reusability. Notably, LacN@Cu/pHAP-BC retained 80.15% of its initial activity after 10 cycles, while LacN@Cu/nHAP-BC maintained 71.98%. Their physicochemical properties can explain this difference.

BET analysis revealed that Cu/pHAP-BC had a higher specific surface area (179.1 m^2/g) than Cu/nHAP-BC (168.9 m^2/g), providing more anchoring sites for LacN attachment. The biochar derived from rape straw also contributed to the alkaline microenvironment, protecting the enzyme from acidic damage.

High temperatures easily disrupt protein structures, thereby reducing catalytic activity or causing permanent inactivation [36]. The strong bonding within the LacN structure and the confinement by the Cu/HAP-BC support reduce enzyme mobility and enhance its thermal stability. Figure 7d compares the thermostability of free laccase and LacN@Cu/HAP-BC from 25 to 75 °C. The immobilized laccase showed significantly improved stability; at 45 °C (the optimal temperature for both), free laccase retained only 45.05% of its activity, whereas the composites remained largely unaffected. Although activity declined for both forms at higher temperatures, LacN@Cu/HAP-BC exhibited a much slower decay rate. Free laccase was completely inactivated at approximately 70 °C, whereas LacN@Cu/nHAP-BC and LacN@Cu/pHAP-BC retained 15.01% and 10.73% of their activity even at 75 °C, respectively. This superior thermotolerance is attributed to the "nanoflower" structure and immobilization, which restrict protein mobility and protect the tertiary structure from thermal denaturation.

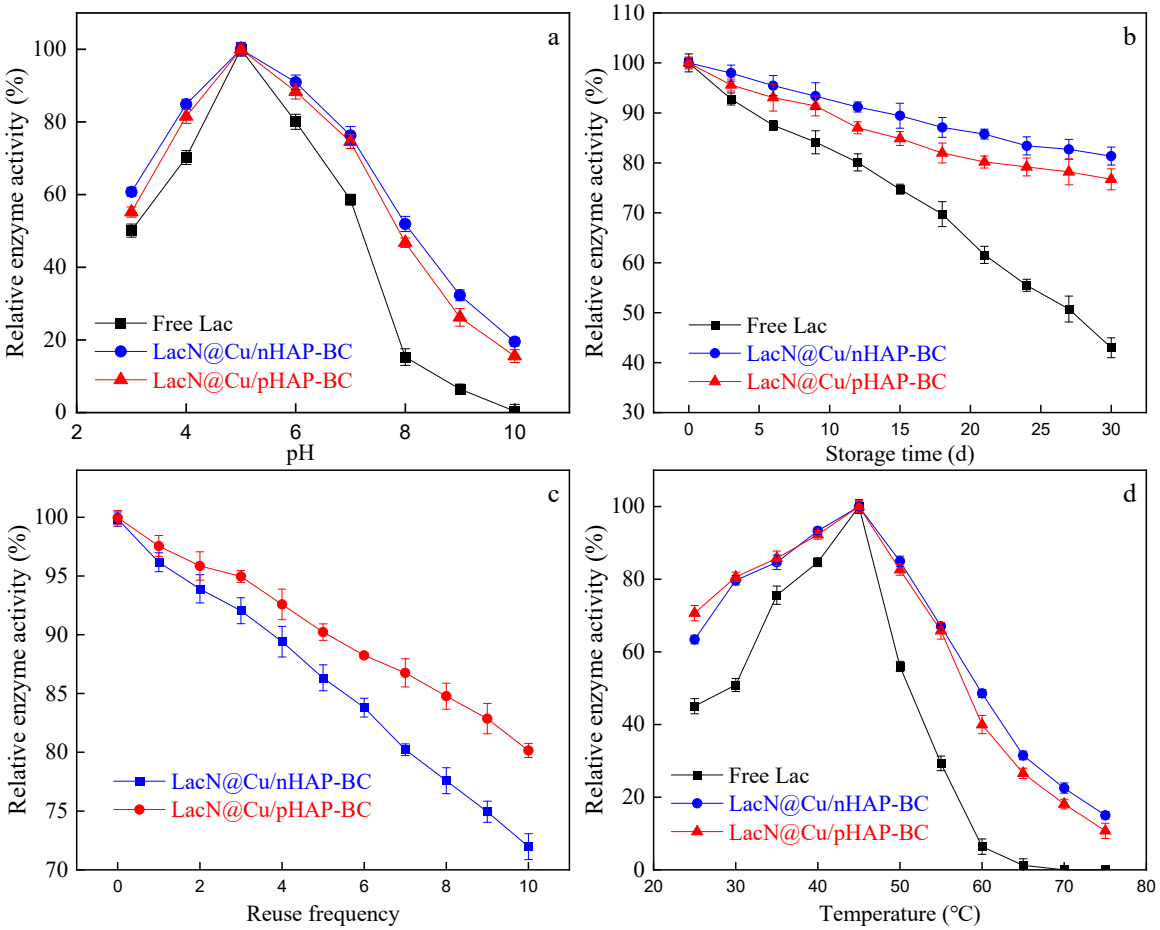

Figure 7. (**a**) The pH stability of free laccase and LacN@Cu/HAP-BC; (**b**) The storage stability of free laccase and LacN@Cu/HAP-BC; (**c**) Reuse stability of LacN@Cu/HAP-BC; (**d**) The thermal stability of free laccase and LacN@Cu/HAP-BC.

3.5.2. Heat Tolerance and Inactivation Kinetics

To further investigate thermal tolerance, the residual activities of LacN@Cu/HAP-BC and an equivalent amount of free laccase were monitored at 65 °C Figure 8a. Although all samples exhibited a declining trend over 120 min, the free laccase deactivated much faster. At the end of the incubation, free laccase retained only 56.00% of its initial activity, whereas LacN@Cu/HAP-BC maintained

significantly higher activity, confirming that immobilization enhances stability. At high temperatures, enzymes are prone to thermal unfolding, which exposes reactive groups and hydrophobic regions, leading to protein aggregation and conformational changes that result in inactivation. The thermal inactivation curves and their corresponding fits are presented in Figure 8b.

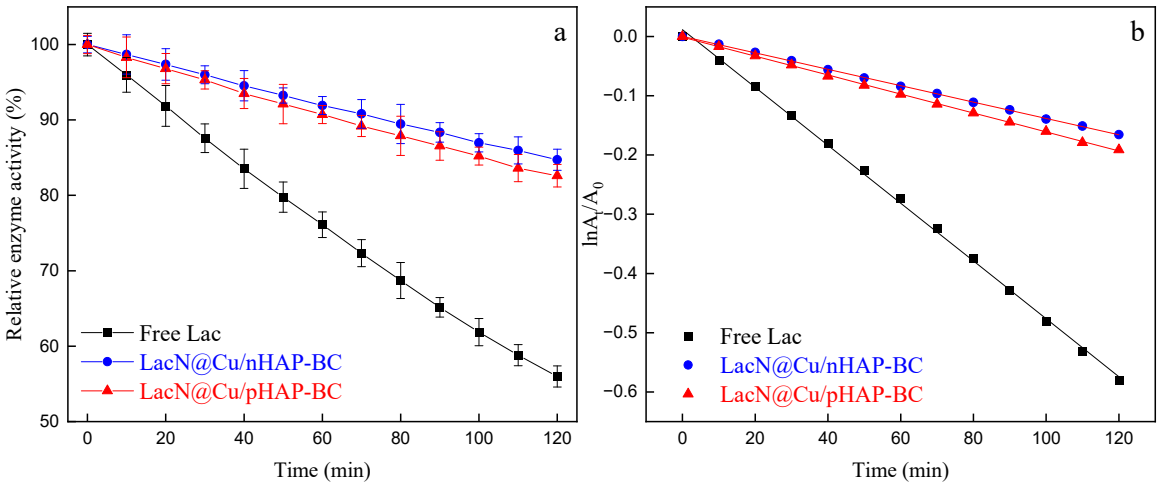

Figure 8. Thermal tolerance and thermal inactivation mechanics of free laccase and LacN@Cu/HAP-BC: (**a**) Changes of relative enzyme activity with time; (**b**) Mechanical fitting curve of thermal deactivation.

The thermal deactivation kinetic parameters derived from the fitted curves are summarized in Table 2, which includes the deactivation rate constant (k), half-life ($t_{1/2}$), and R^2 values. The high R^2 values indicate a satisfactory fit for all samples, confirming that their thermal deactivation follows a first-order kinetic model. Specifically, the half-life of free laccase was determined to be 142 min, whereas LacN@Cu/nHAP-BC and LacN@Cu/pHAP-BC exhibited significantly longer half-lives of 502 min and 433 min, respectively. The half-life of LacN@Cu/HAP-BC was approximately 3.0–3.5 times that of free laccase. This suggests that the LacN structure, combined with the pore shielding effect of Cu/HAP-BC, effectively protects the protein structure of laccase molecules, thereby enhancing their thermal stability.

Table 2. Thermal activity mechanics parameters.

Parameter	Free Laccase	LacN@Cu/nHAP-BC	LacN@Cu/pHAP-BC
Intercept	−0.0049	−0.0014	−0.0016
Slope	0.012	0.000096	−0.0011
R^2	0.9991	0.9998	0.9996
k (min^{-1})	0.0049	0.0014	0.0016
$t_{1/2}$(min)	142	502	433

3.5.3. Comparison of Enzyme Stability Parameters

Table 3 compares the stability parameters of different immobilized laccase systems, defined as the conditions under which the relative activity remains above 50%. It can be observed that the as-prepared LacN@Cu/HAP-BC retained high storage stability for up to 30 d. In contrast, immobilized laccase prepared using MOF materials or calcium/copper alginate beads maintained relative activities above 50% for only 10 d or 21 d, respectively. Regarding pH stability, most immobilized laccases listed in Table 2 maintained favorable activity within the range of pH 3.0–8.0. This is attributed to the fact that while the optimal pH of free laccase is typically 3.0–5.0, the immobilization process effectively broadens its applicability under alkaline conditions. The LacN@Cu/HAP-BC prepared in this study maintained over 50% relative activity within the range of pH 3.0–8.0, demonstrating comparable acid-base stability to

other systems, whereas the immobilized laccase prepared using polyacrylamide-alginate cryogels was limited to a narrower range of pH 2.5–4.0. For thermal stability, the operating ranges were similar among the listed materials, generally maintaining >50% activity between 20–60 °C, with only calcium/copper alginate beads and PVDF/MWCNT membranes achieving a maximum thermal tolerance of 70 °C. Notably, the LacN@Cu/HAP-BC prepared in this study exhibited the best reusability, retaining more than 50% of its relative activity even after 10 reaction cycles. Overall, in comparison with similar immobilized laccase systems, LacN@Cu/HAP-BC demonstrates superior stability performance.

Table 3. Comparison of stability parameters for different immobilized laccases.

Support	**Polyacrylonitrile Biochar**	**Pine Wood Nanobiochar**	**MOF-Supported Fe_3O_4**	**Calcium/Copper Alginate Beads**	**PVDF/MWCNT Membrane**	**Alginate Cryogel**	**Cu/HAP-BC**
Laccase source	*Trametes versicolor*	*Trametes versicolor*	*B. amyloliquefaciens LC02*	*Cyberlindnera fabianii*	*Trametes hirsuta*	*Trametes versicolor*	*Trametes versicolor*
Storage stability	>30 d	25 d	>10 d	>21 d	-	-	>30 d
pH stability	3.0~8.0	3.0~5.0	-	3.0~9.0	-	2.5~4.0	3.0~8.0
Thermal stability	20~60 °C	20~60 °C	20~80 °C	30~70 °C	20~70 °C	30~70 °C	30~60 °C
Reusability	6	3	5	3	2	7	10
Reference	[37]	[38]	[39]	[40]	[41]	[42]	This work

Despite the excellent reusability and storage stability of the developed LacN@Cu/HAP-BC composites, a gradual loss of residual activity was observed after ten consecutive reuse cycles. Several factors may account for this decline, including desorption of surface-loaded LacN nanoflowers, trace copper leaching, pore blockage by catalytic intermediates, and irreversible protein denaturation [43,44]. Among these, the gradual detachment of partially immobilized LacN from the carrier surface is considered the most likely primary cause, consistent with general observations in enzyme immobilization studies. Nevertheless, the composites remain highly promising for practical bioresource and environmental applications. Their high storage stability and reusability render them suitable for continuous-flow packed-bed bioreactors in wastewater treatment or lignocellulosic biomass pretreatment. Furthermore, the use of low-cost, waste-derived materials (e.g., porcine bone and rape straw) aligns well with the circular bioeconomy concept and facilitates scalability. To advance toward real-world implementation, future research should focus on (1) application to real industrial wastewater containing mixed refractory pollutants such as chlorophenols and bisphenol A, (2) scale-up studies in continuous-flow packed-bed bioreactors, and (3) systematic economic analysis of the entire immobilization and operation process. The robust performance data obtained in the present work—including 10-cycle reusability and 30-day storage stability—provide a solid preliminary foundation for these subsequent investigations.

4. Conclusions

This study successfully constructed highly stable and reusable laccase biocatalysts by immobilizing laccase-inorganic hybrid nanoflowers (LacN) onto two copper-doped hydroxyapatite/biochar supports (Cu/nHAP-BC and Cu/pHAP-BC), with preparation conditions systematically optimized via single-factor tests and Box–Behnken response surface methodology to ensure high catalytic activity and firm binding. Structural characterizations confirmed that flower-like LacN was firmly anchored on the porous supports, with well-preserved HAP crystallinity and multivalent copper sites that enhance electron transfer and protect the enzyme from conformational damage. Kinetic analysis revealed elevated K_m and reduced v_{max} in the immobilized systems, attributable to moderate diffusion resistance

and steric effects from the carrier, yet the synergistic catalytic contribution of copper active sites compensated for the slight loss in substrate affinity, maintaining favorable overall efficiency. The composite catalysts exhibited outstanding comprehensive performance: after 30 d of storage, LacN@Cu/nHAP-BC and LacN@Cu/pHAP-BC retained 81.35% and 76.70% of their initial activities, respectively, while their thermal half-lives at 65 °C were 3.0–3.5 times longer than that of free laccase; moreover, they maintained high relative activity over 10 consecutive reuse cycles, outperforming most reported immobilized laccase systems. This synergistic strategy effectively overcomes the poor stability of free laccase and the difficulty of recovering pure LacN, while using waste-derived raw materials reduces costs and enhances environmental friendliness. Collectively, these findings establish LacN@Cu/HAP-BC as a low-cost, readily accessible, and highly stable biocatalytic candidate for environmental remediation. Future work will focus on evaluating its performance in continuous-flow packed-bed bioreactors and its degradation efficiency toward real refractory pollutants in complex industrial wastewater matrices, alongside techno-economic assessment of the entire immobilization and operation process to facilitate industrial translation.

Supplementary Materials

The following supporting information can be found at: https://www.sciepublish.com/article/pii/1215, Table S1: Experiment design parameters; Table S2: Box Behnken response surface methodology coding table; Table S3: Parameter values of different models; Table S4: Parameter values under quadratic equation model; Table S5: Bet parameters of catalyst.

Acknowledgements

The authors would like to thank Shiyanjia Lab (www.shiyanjia.com) for the characterization support.

Author Contributions

Conceptualization, Z.W. and D.R.; Methodology, Z.W.; Validation, Z.W., D.R. and R.C.; Formal Analysis, Z.W.; Investigation, Z.W.; Resources, D.R. and R.C.; Data Curation, Z.W.; Writing—Original Draft Preparation, Z.W.; Writing—Review & Editing, Z.W., D.R. and R.C.; Visualization, Z.W.; Supervision, D.R. and R.C.; Project Administration, Z.W., D.R. and R.C.; Funding Acquisition, Z.W. All authors have read and agreed to the published version of the manuscript.

Ethics Statement

Not applicable.

Informed Consent Statement

Not applicable.

Data Availability Statement

The original contributions presented in this study are included in the article and the Supplementary Materials.

Funding

This research was funded by the National Natural Science Foundation of China (Grant No. 41571306 and 52604629) and the Natural Science Foundation of Hubei Province (Grant No. 2025AFD245).

Declaration of Competing Interest

The authors declare that they have no known competing financial interests or personal relationships that could have appeared to influence the work reported in this paper.

References

1. Zhao H, Zhao Y, Wang Y, Xiao G, Su H. Adsorption and High-Value Transformation of Volatile Fatty Acids from Microbial Fermentation Products: A Review. *Green Chem. Technol.* **2025**, *2*, 10001. DOI:10.70322/gct.2025.10001
2. Ghattavi S, Homaei A. Marine enzymes: Classification and application in various industries. *Int. J. Biol. Macromol.* **2023**, *230*, 123136. DOI:10.1016/j.ijbiomac.2023.123136
3. Ge J, Lei J, Zare RN. Protein–inorganic hybrid nanoflowers. *Nat. Nanotechnol.* **2012**, *7*, 428–432. DOI:10.1038/nnano.2012.80
4. Zhang M, Zhang Y, Yang C, Ma C, Tang J. Enzyme-inorganic hybrid nanoflowers: Classification, synthesis, functionalization and potential applications. *Chem. Eng. J.* **2021**, *415*, 129075. DOI:10.1016/j.cej.2021.129075
5. Wang H, Tang L-X, Ye Y-F, Ma J-X, Li X, Si J, et al. Laccase immobilization and its degradation of emerging pollutants: A comprehensive review. *J. Environ. Manag.* **2024**, *359*, 120984. DOI:10.1016/j.jenvman.2024.120984
6. Gupta RK, Patel SKS, Lee J-K. Novel cofactor regeneration-based magnetic metal–organic framework for cascade enzymatic conversion of biomass-derived bioethanol to acetoin. *Bioresour. Technol.* **2024**, *408*, 131175. DOI:10.1016/j.biortech.2024.131175
7. Wang Z, Ren D, Jiang S, Yu H, Cheng Y, Zhang S, et al. The study of laccase immobilization optimization and stability improvement on CTAB-KOH modified biochar. *BMC Biotechnol.* **2021**, *21*, 47. DOI:10.1186/s12896-021-00709-3
8. Wang Z, Ren D, Yu H, Zhang S, Zhang X, Chen W. Preparation optimization and stability comparison study of alkali-modified biochar immobilized laccase under multi-immobilization methods. *Biochem. Eng. J.* **2022**, *181*, 108401. DOI:10.1016/j.bej.2022.108401
9. Wang Z, Ren D, Zhao Y, Huang C, Zhang S, Zhang X, et al. Remediation and improvement of 2,4-dichlorophenol contaminated soil by biochar-immobilized laccase. *Environ. Technol.* **2021**, *42*, 1679–1692. DOI:10.1080/09593330.2019.1677782
10. Wang Z, Ren D, Cheng Y, Zhang X, Zhang S, Chen W. Immobilization of laccase on chitosan functionalized halloysite nanotubes for degradation of Bisphenol A in aqueous solution: degradation mechanism and mineralization pathway. *Heliyon* **2022**, *8*, e09919. DOI:10.1016/j.heliyon.2022.e09919
11. Wang Z, Ren D, Zhang X, Zhang S, Chen W. Adsorption-degradation of malachite green using alkali-modified biochar immobilized laccase under multi-methods. *Adv. Powder Technol.* **2022**, *33*, 103821. DOI:10.1016/j.apt.2022.103821
12. Wang Z, Ren D, Wu J, Jiang S, Yu H, Cheng Y, et al. Study on adsorption-degradation of 2,4-dichlorophenol by modified biochar immobilized laccase. *Int. J. Environ. Sci. Technol.* **2022**, *19*, 1393–1406. DOI:10.1007/s13762-021-03151-2
13. Jiang S, Ren D, Wang Z, Zhang S, Zhang X, Chen W. Improved stability and promoted activity of laccase by One-Pot encapsulation with Cu (PABA) nanoarchitectonics and its application for removal of Azo dyes. *Ecotoxicol. Environ. Saf.* **2022**, *234*, 113366. DOI:10.1016/j.ecoenv.2022.113366
14. Jiang S, Wang Z, Qin Y, Cao B, Chi R. Eco-Friendly Synthesis of Spherical Lanthanum-Doped Hydroxyapatite from Phosphogypsum Waste: A High-Efficiency Strategy for Fluoride Removal in Aqueous Solutions. *Green Chem. Technol.* **2026**, *3*, 10008. DOI:10.70322/gct.2026.10008
15. Ding T, Chi R, Yu J, Yin W, Hu Z, Zhao Q. Synthesis of Hydroxyapatite Porous Microspheres for Efficient Adsorption of Copper Ion from Water. *Green Chem. Technol.* **2026**, *3*, 10011. DOI:10.70322/gct.2026.10011
16. Liu Y, Fan C, Zhang B, Wen B, Zhang L. The Crystal Structure of Apatite and Copper-Doped Apatite. *Green Chem. Technol.* **2025**, *2*, 10005. DOI:10.70322/gct.2025.10005
17. Wang Z, Ren D, Shang S, Zhang S, Zhang X, Chen W. Novel synthesis of Cu-HAP/SiO2@carbon nanocomposites as heterogeneous catalysts for Fenton-like oxidation of 2,4-DCP. *Adv. Powder Technol.* **2022**, *33*, 103509. DOI:10.1016/j.apt.2022.103509
18. Wang M, Ren D, Wang Z, Li Y, Zhang S, Gong X, et al. A novel Cu/HAP@sBC composite as a persulfate activator for the removal of 2,4,6-trichlorophenol. *Catal. Commun.* **2023**, *184*, 106793. DOI:10.1016/j.catcom.2023.106793
19. Wang Z, Ren D, Chi R. Synthesis of copper-based Fenton-like catalyst (Cu/HAP-sBC) for oxidative degradation of p-nitrophenol in aqueous solution. *J. Mol. Struct.* **2025**, *1339*, 142383. DOI:10.1016/j.molstruc.2025.142383

20. Akram W, Garud N. Design expert as a statistical tool for optimization of 5-ASA-loaded biopolymer-based nanoparticles using Box Behnken factorial design. *Futur. J. Pharm. Sci.* **2021**, *7*, 1–17. DOI:10.1186/s43094-021-00299-z
21. Martin E, Audonnet F, Yaacoub D, Dubessay P, Michaud P. Nernst-Michaelis-Menten framework unlocks electrochemical kinetics for laccases. *Bioelectrochemistry* **2025**, *165*, 109003. DOI:10.1016/j.bioelechem.2025.109003
22. Costa JB, Lima MJ, Sampaio MJ, Neves MC, Faria JL, Morales-Torres S, et al. Enhanced biocatalytic sustainability of laccase by immobilization on functionalized carbon nanotubes/polysulfone membranes. *Chem. Eng. J.* **2019**, *355*, 974–985. DOI:10.1016/j.cej.2018.08.178
23. Wu X, Ge J, Hou M. Metal-organic frameworks and inorganic nanoflowers: A type of emerging inorganic crystal nanocarrier for enzyme immobilization. *Catal. Sci. Technol.* **2015**, *5*, 5077–5085. DOI:10.1039/C5CY01181G
24. Vo TN, Tran TD, Nguyen HK, Kong DY, Kim MI, Kim IT. *In situ* growth of hybrid nanoflowers on activated carbon fibers as electrodes for mediatorless enzymatic biofuel cells. *Mater. Lett.* **2020**, *281*, 128662. DOI:10.1016/j.matlet.2020.128662
25. Dlamini ML, Lesaoana M, Kotze I, Richards HL. Zeolitic imidazolate frameworks as effective crystalline supports for aspergillus-based laccase immobilization for the biocatalytic degradation of carbamazepine. *Chemosphere* **2023**, *311*, 137142. DOI:10.1016/j.chemosphere.2022.137142
26. Rong J, Zhang T, Qiu F, Zhu Y. Preparation of Efficient, Stable, and Reusable Laccase–$Cu_3(PO_4)_2$ Hybrid Microspheres Based on Copper Foil for Decoloration of Congo Red. *ACS Sustain. Chem. Eng.* **2017**, *5*, 4468–4477. DOI:10.1021/acssuschemeng.7b00820
27. Li X, Wu Z, Tao X, Li R, Tian D, Liu X. Gentle one-step co-precipitation to synthesize bimetallic CoCu-MOF immobilized laccase for boosting enzyme stability and Congo red removal. *J. Hazard. Mater.* **2022**, *438*, 129525. DOI:10.1016/j.jhazmat.2022.129525
28. Yuan Y, Cai W, Xu J, Cheng J, Du, K.-S., Recyclable laccase by coprecipitation with aciduric Cu-based MOFs for bisphenol A degradation in an aqueous environment. *Colloids Surf. B Biointerfaces* **2021**, *204*, 111792. DOI:10.1016/j.colsurfb.2021.111792
29. Zapata-Castillo P, Villalonga-Santana L, Islas-Flores I, Rivera-Muñoz G, Ancona-Escalante W, Solís-Pereira S. Synergistic action of laccases from Trametes hirsuta Bm2 improves decolourization of indigo carmine. *Lett. Appl. Microbiol.* **2015**, *61*, 252–258. DOI:10.1111/lam.12451
30. Han Z, Fan X, Yu S, Li X, Wang S, Lu L. Metal-organic frameworks (MOFs): A novel platform for laccase immobilization and application. *J. Environ. Chem. Eng.* **2022**, *10*, 108795. DOI:10.1016/j.jece.2022.108795
31. Zhang K, Yang W, Liu Y, Zhang K, Chen Y, Yin X. Laccase immobilized on chitosan-coated Fe_3O_4 nanoparticles as reusable biocatalyst for degradation of chlorophenol. *J. Mol. Struct.* **2020**, *1220*, 128769. DOI:10.1016/j.molstruc.2020.128769
32. Patel SKS, Gupta RK, Karuppanan KK, Padhi DK, Ranganathan S, Paramanantham P, et al. Trametes versicolor Laccase-Based Magnetic Inorganic-Protein Hybrid Nanobiocatalyst for Efficient Decolorization of Dyes in the Presence of Inhibitors. *Materials* **2024**, *17*, 1790. DOI:10.3390/ma17081790
33. da Silva CKH, Polidoro AS, Ruschel PMC, Thue PS, Jacques RA, Lima ÉC, et al. Laccase covalently immobilized on avocado seed biochar: A high-performance biocatalyst for acetaminophen sorption and biotransformation. *J. Environ. Chem. Eng.* **2022**, *10*, 107731. DOI:10.1016/j.jece.2022.107731
34. Patel SKS, Gupta RK, Kim S-Y, Kim I-W, Kalia VC, Lee J-K. Rhus vernicifera laccase immobilization on magnetic nanoparticles to improve stability and its potential application in bisphenol A degradation. *Indian J. Microbiol.* **2021**, *61*, 45–54. DOI:10.1007/s12088-020-00912-4
35. Zdarta J, Jankowska K, Wyszowska M, Kijeńska-Gawrońska E, Zgoła-Grześkowiak A, Pinelo M, et al. Robust biodegradation of naproxen and diclofenac by laccase immobilized using electrospun nanofibers with enhanced stability and reusability. *Mater. Sci. Eng. C* **2019**, *103*, 109789. DOI:10.1016/j.msec.2019.109789
36. Panwar V, Lzaod S, Dutta T. Thermostable Bacterial Laccase: Catalytic Properties and Its Application in Biotransformation of Emerging Pollutants. *ACS Omega* **2023**, *8*, 34710–34719. DOI:10.1021/acsomega.3c03627
37. Taheran M, Naghdi M, Brar SK, Knystautas EJ, Verma M, Surampalli RY. Degradation of chlortetracycline using immobilized laccase on Polyacrylonitrile-biochar composite nanofibrous membrane. *Sci. Total Environ.* **2017**, *605*, 315–321. DOI:10.1016/j.scitotenv.2017.06.185
38. Naghdi M, Taheran M, Brar SK, Kermanshahi-pour A, Verma M, Surampalli RY. Pinewood nanobiochar: A unique carrier for the immobilization of crude laccase by covalent bonding. *Int. J. Biol. Macromol.* **2018**, *115*, 563–571. DOI:10.1016/j.ijbiomac.2018.04.105

39. Wang J, Yu S, Feng F, Lu L. Simultaneous purification and immobilization of laccase on magnetic zeolitic imidazolate frameworks: Recyclable biocatalysts with enhanced stability for dye decolorization. *Biochem. Eng. J.* **2019**, *150*, 107285. DOI:10.1016/j.bej.2019.107285
40. Olajuyigbe FM, Adetuyi OY, Fatokun CO. Characterization of free and immobilized laccase from Cyberlindnera fabianii and application in degradation of bisphenol A. *Int. J. Biol. Macromol.* **2019**, *125*, 856–864. DOI:10.1016/j.ijbiomac.2018.12.106
41. Masjoudi M, Golgoli M, Nejad ZG, Sadeghzadeh S, Borghei SM. Pharmaceuticals removal by immobilized laccase on polyvinylidene fluoride nanocomposite with multi-walled carbon nanotubes. *Chemosphere* **2021**, *263*, 128043. DOI:10.1016/j.chemosphere.2020.128043
42. Yavaşer R, Karagözler AA. Laccase immobilized polyacrylamide-alginate cryogel: A candidate for treatment of effluents. *Process Biochem.* **2021**, *101*, 137–146. DOI:10.1016/j.procbio.2020.11.021
43. Hu W, Zong J, Gong J, Xue R, Lv Y, Liu B, et al. Lipase immobilization via dynamic defect-engineered ZIF-8: A bioactivity-enhanced platform for high-efficiency screening of herbal lipase inhibitors. *Int. J. Biol. Macromol.* **2025**, *335*, 149264. DOI:10.1016/j.ijbiomac.2025.149264
44. Zhao Q, Zhang X, Wang S, Deng L, Bai Y, Du K. Robust and Versatile OPH-Cu Phosphate Hybrid Nanoflower for Organophosphorus Compound Degradation. *J. Agric. Food Chem.* **2025**, *73*, 18210–18219. DOI:10.1021/acs.jafc.5c03908